Available online at http://ijim.srbiau.ac.ir/
Int. J. Industrial Mathematics (ISSN 2008-5621)
Vol. 14, No. 3, 2022 Article ID IJIM-1413, 12 pages
DOI: http://dx.doi.org/10.30495/ijim.2022.19651
Research Article

Science and Research Branch (IAU)

Experimental Study and Comparison of a Few Lean (gasoline-natural gas) Dual Fuels Based on Safe Optimum Spark Advance

S. K. Yekani *†, E. Abdi Aghdam ‡, M. Sarabi §

Received Date: 2020-01-28 Revised Date: 2021-02-02 Accepted Date: 2021-11-28

Abstract

Strong dependence of the humans daily life on the engine-powered vehicles, increasing environmental pollutions, especially in urban areas, and reduction of the world oil resources have challenged the energy researchers to make appropriate decisions at regional scale for selecting alternative fuels to improve the engine efficiency and fuel economy. In the current work, the lean-burn idea jointed to dual (gasoline-NG) fuel has been considered to develop the SI engines. To investigate the performance and exhaust gas emissions, experimental tests were performed using a single-cylinder research engine with gasoline-NG dual fuels, including four mass-based blends of the two fuels (G100, G87.5, G75, and G62.5 containing gasoline at 100%, 87.5%, 75%, and 62.5%, respectively, with the remaining part being composed of NG), at 1800 rpm ES and 0.9 ER under at least seven different SAs. The result showed that increasing the NG fraction in the fuel blend, both the and COV of imep decreased. It was implicitly observed that, for blended fuels, non-uniform distribution of each fuel can serve as a new source for cyclic variations. Under the considered lean burning condition at optimal safe SA, the imep and output torque for the gas-contained fuel blends were comparable to those obtained by the pure gasoline. Also, it was detected that an increase in the CR reduced the emitted amounts of HC and CO pollutants.

Keywords : Dual fuel SI engine; Gasoline; Natural gas; Optimum Spark Advance; Emissions; Lean-burn.

1 Introduction

In the recent past decades, the large dependence of the daily life of humans on the engine-powered vehicles in the transportation, traveling, agricultural, and industrial applications has been abundant clear. The increased demand for such engine-powered equipments has added to the volume of pollutant gases, especially in urban areas, thereby contributing to environmental pollution.

*Corresponding author. S.K.Yekani@uma.ac.ir, Tel:+98(45)31500000.
†Department of Mechanical Engineering, Faculty of Engineering, University of Mohaghegh Ardabili, Ardabil, Iran.
‡Department of Mechanical Engineering, Faculty of Engineering, University of Mohaghegh Ardabili, Ardabil, Iran.
§Department of Mechanical Engineering, Faculty of Engineering, University of Mohaghegh Ardabili, Ardabil, Iran.

On the other hand, the decrease in the oil reserves around the world and the need for supplying the input energy for such engines have challenged the energy researchers to make appropriate decisions at regional scale for selecting alternative fuels to improve the engine efficiency and fuel economy. An efficient and novel approach to this challenge is to either replace the fuel with an alternative fuel with lower emissions or use dual fuels. Using combination of two fuels with different fractions can provide a wide spectrum of dual fuels. With vast reserves of natural gas (NG) [?] along with the largest number of NG- fueled vehicles in the world, Iran has large potentials for using the NG as a fuel. This has drawn attention from the researchers in the fields of energy and engine design [?]. Application of NG in a spark-ignition engine offers a number of advantages, including lower tendency to knock compared to with the conventional fossil fuels, potential for increasing the compression ratio (CR), easy mixing with air, reduced emission, and economic gain [?]. In many cases, the NG is simply used to fuel an originally gasoline-based engine. However, due to the lower burning velocity and attenuated volumetric efficiency of the fuel because of its gaseous nature, the output power of the engine is affected. Moreover, appreciating the advantages offered by the NG, bi-fuel gasoline-NG engines have been frequently used in the recent past. A key feature of a bi-fuel engine is that the user can selectively opt for either NG or gasoline. In the meantime, the design and control of the auxiliary systems for such bi-fuel engines is are faced by particular complexities and problems, because most of such engines have been originally designed for gasoline as the base fuel [?, ?]. Considering the drawbacks of using either the gasoline or the NG alone in a spark-ignition engine, the idea of using a combination of the two fuels for improving the engine performance while reducing the emissions has been emerged [?, ?]. The fuel combination can lead to lower tendency to knocking, as compared to the gasoline. The idea of lean-burn in engine, introduced to achieve economic saving and reduce the emissions during the last two decades, can be accompanied by the dual fuel development. The advantage of the lean mixture in terms of reduced tendency to knock and the problem of increased cyclic variations can develop into another challenge. The inappropriate combustion limit of a lean mixture is related to the engine design, besides the fuel type. In this respect, Run et al. [?] investigated the incomplete combustion threshold in an engine operating at 1200 rpm for three low-emission alternative fuels, namely NG, alcohol, and syngas. Their results showed that, among the conventional fuels, the NG exhibited a lower incomplete combustion limit compared to gasoline and alcohol.

Based on the fuel phase, the dual fuels can be categorized under either of three primary categories, namely liquid-liquid, liquid-gas, and gas-gas combined fuels, with different fuel- delivery requirements for different categories though common-phase cases may end up with simple requirements. In the recent research works, various dual fuels have been investigated, namely gasoline-ethanol [?, ?], gasoline-normal butanol [?], gasoline-LPG [?], gasoline- NG [?, ?, ?, ?, ?, ?] and methanol-hydrogen [?], for spark-ignition engines. Several studies have considered four-cylinder commercial engines [?, ?, ?], where the user might occasionally fail to stabilize the ER and undertake SA, SA, management. Moreover, the four- cylinder nature of the engine in such studies might question the accuracy of the results due to possible inconsistencies in the blend quality, combustion products, and heat transfer within different cylinders as well as the possible slippage of the SA of different cylinders as a result of elastic angular deformation of the crankshaft under the mechanical load. Therefore, the authors believed that accurate research works can be done conducted on special single- cylinder engines with use-adjustable parameters.

Pipiten et al. [?] evaluated the effect of simultaneous injection of gasoline and NG in a commercial four-cylinder SI engine, as compared to the case with gasoline as single fuel. Their results revealed that the tendency to knock was lower with the dual fuel rather than the pure gasoline, and the SA slightly retarded. In their work, the engine characteristics and operating conditions were in such a way that the comparisons were made without equalizing the ER, so that the tests with gasoline alone were performed at ER=1.11-1.19 while the experiments with dual fuel were conducted at stochiometric mixtures. Movahed et al. [?] performed an experimental research on a fully loaded turbo-charged engine and showed that, with increasing the NG fraction in the dual case, the CO and HC emissions decreased.

Performance of a dual fuel in a SI engine can be different depending on the dominant fuel type. In an experimental study on a gasoline-NG dual fueled SI engine with NG as the dominance fuel, Ramasami et al. [?] compared the exhaust emission and engine performance between the pure fuel (NG) and dual fuel, and showed that an increase in the gasoline fraction of the blend led to increased output torque though the emitted HCs increased for most part, as compared to the base case (NG). DLourier et al. [?] studied a single-cylinder SI gasoline-NG dual fuel engine with direction injection and NG and gasoline manifold and captured slow-motion videos from within the combustion chamber. They showed that the development of the flame front goes faster with the dual fuel rather than pure NG, and that under stochiometric conditions, the coefficient of variation (COV) in indicated mean effective pressure (imep) decreased with increasing the NG fraction. In a recent contribution, Behrad et al. [?] investigated the knocking characteristics of a single-cylinder spark-ignition engine fueled by a few blended fuels that were dominantly composed of gasoline by measuring the cylinder pressure and filtering theirs knocking signals. Sarabi and Abdi-Aghdam [?] examined the performance and emission characteristics of a dual-fueled (gasoline-NG) SI engine under stoichiometric conditions. The knocking and lean burning conditions were out of scope of their research.

Based on the review of the open-access literature, it was found that the lean-burn gasoline-NG dual-fueled SI engines are yet to be addressed adequately. The present research considers four different combinations of gasoline with NG (with the gasoline as the dominant constituent), performance and emission characteristics of a single-cylinder research engine were evaluated under lean condition at an ER of 0.9, 1800 rpm ES, and two CRs, namely 10 and 11. On a mass basis, the studied blends contained gasoline at 100% (G100), 87.5% (G87.5), 75% (G75), and 62.5% (G62.5), with the remaining part of the blend been composed of NG. The study was performed in the non-knocking region.

2 Experimental setup

The apparatus used in this work was composed of a CT300 test stand (G.U.N.T. Gertebau GmbH, Germany) on which a single-cylinder SI engine was mounted. This research engine was coupled with a speed-adjustable synchronized dynamometer. Following a series of research works, the fuel injection system was changed from a mechanical carburetor system to an electronic dual fuel (gasoline and NG) injection system with user-adjustable injection timing and duration for different fuels and spark timing [?, ?, ?], making the engine capable of operating with either gasoline or NG alone or a combination of the both.

In this research, using the fuel delivery system, the gasoline injection pressure was maintained at a gauge pressure of 3.5 bar. In the NG fuel delivery system, the gaseous fuel was depressurized to 2.5 bar upon passing through a regulator installed on a high-pressure (200-250 bar) CNG capsule, before being dispatched through the rail connected to the injector. In this way, independent injection of the two fuels through the injectors connected to the engine intake manifold became possible. At each test, considering the required injection for each injector (injection period), injection timing and spark timing were adjusted by the engine management assembly. Figure **??** shows a flow diagram of the fuel injection control systems. Previous research works have measured and calibrated the effects of the injection period and the injected place pressure under various sets of operating conditions for both gasoline and CNG injectors [?]. Using the obtained correlation equation, the required injection period for each fuel was assessed and applied.

The fast and high-precision measurement sys-

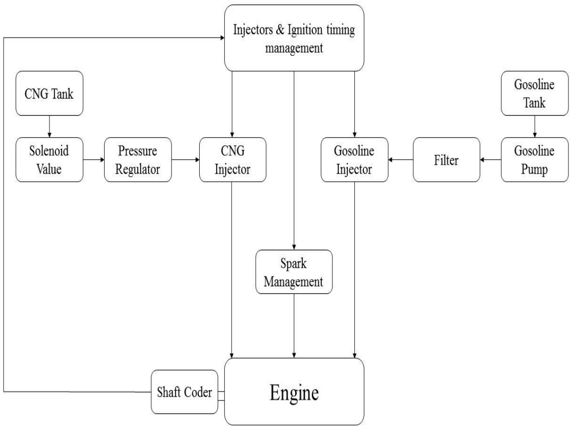

Figure 1: Flow diagram of the fuel injection control and spark timing systems

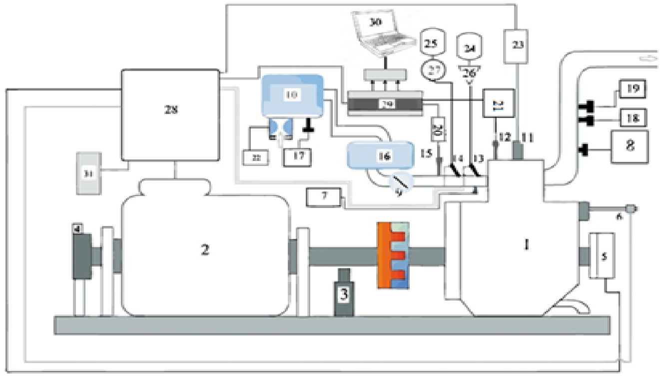

Figure 2: Test platform, control assembly, and measurement systems 1: Engine, 2:dynamometer, 3: engine speed sensor, 4: torque sensor, 5: shaft encoder, 6: suction TDC sensor, 7: inlet mixture temperature sensor,8. exhaust gas temperature sensor, 9: throttle, 10: primary air comfort chamber, 11: spark plug, 12: dynamic pressure transducer, 13: NG injector, 14: gasoline injector, 15: absolute pressure transducer, 16:secondary air comfort chamber, 17:primary comfort tank temperature sensor, 18: gas analyzer a, 19: gas analyzer b, 20: amplifier of the absolute pressure transducer, 21: amplifier of dynamic pressure transducer, 22: inlet air flow sensor, 23: ignition system, 24: NG tank,25: gasoline tank, 26: NG pressure regulator, 27: gasoline pump, 28:engine management system, 29: AD-Logger, 30: PC, 31: electricity input of the system

tems of in-cylinder and intake manifold pressures are essential for analyzing engine combustion. In this research, the in-cylinder pressure signal was measured by a dynamic pressure transducer (Kistler 6025C), with a Kistler 5011B amplifier used to amplify the signal. The intake manifold pressure was measured using a Keller PAA-M5 HB/3bar absolute pressure transducer coupled with the respective amplifier. The crankshaft angle signals were recorded by a Kistler 2613B shaft encoder. A four-channel ADLINK DAQ2005 data logger was utilized to convert analogue signal to digital one (A/D), capable for maximum sampling rate of 500 kHz; the logger was coupled with the respective software to store the data.

Exhaust gas composition (CO, HC, CO2, O2) and the relative air-fuel ratio () were obtained using two gas analyzer apparatuses, namely a Saxon Infralyt-CL and a Testo 350XL. Specifications of the utilized research engine are briefly presented in Table **??**. Figure **??** demonstrates the test platform, control assembly, and measurement systems schematically.
In this investigation, the NG composition described in Table **??** (based on the volumetric percentages of different species [?] with the average chemical formula $C_{1.04}H_{3.97}$ for the HC part was used. About 94.91% of the total NG was composed of HC, with the remaining part being made up of impurities in the form of CO_2 and N_2. Average chemical formula of the gasoline was assumed $C_{7.76}H_{13.1}$ with a density of 746 $kg.m^{-3}$ [?]. Assuming that the volumetric fraction is identical to the molar fraction for the NG, the stoichiometric equation of the air-dual fuel (gasoline-NG) mixture could be written as Equation (**??**):

$$\tilde{x}C_{7.76}H_{13.1} + (1-\tilde{x})(0.9491C_{1.04}H_{3.97} + 0.00694CO_2 + 0.045N_2) + \alpha_s(O_2 + 3.76N_2 + \varpi) \quad (2.1)$$

Table 1: Specifications of the CT300 research engine

Specification	Description
Cylinder diameter	90 mm
Piston course	74 mm
Displaced volume	470 cm^3
CR	10, 11
Ignition system	Spark timing-adjustable electronic
Fueling system	NG- and gasoline-fueled injection
Lubrication system	Compressive-spray
Cooling system	Single-flow water-cooled
Number and position of valves	2 OHV
Intake valve opening and closing angles	Opening at 0° TDC and closing at 50° aBDC
Outlet value opening and closing angles	Opening at 40° bBDC, closing at 8° aTDC
Respiration mode	Natural

Table 2: Composition of the natural gas [?]

Constituent	Percent
CH_4	88.323%
C_2H_6	4.672 %
C_3H_3	1.137 %
C_4H_{10}	0.484 %
C_5H_{12}	0.181 %
CO_2	0.694 %
N_2	4.5 %
H_2S	0.849 ppm

where $\tilde{x}$ is the molar fraction of the gasoline in the dual fuel, α_s is the required number of moles of oxygen in the stoichiometric mixture per mole of the dual fuel, and ϖ is the number of moles of H_2O per mole of O_2 in the air. Using the molar mass of the air (Mair) and the molecular mass of the water (MH_2O), the value of ϖ could be obtained through Equation (**??**):

$$\varpi = \frac{4.76 \times M_{air}}{M_{H_2O}}\omega \tag{2.2}$$

where ω is the moisture ratio (i.e. mass of water vapor per unit mass of dry air). The average molecular masses of gasoline (M_G) and natural gas (M_{NG}) were utilized to obtain the relation between the molar ($\bar{x}$) and mass (x) fractions of the gasoline in the dual fuel, using Equation (**??**):

$$\tilde{x} = \frac{xM_{NG}}{(1-x)M_G + M_{NG}x} \tag{2.3}$$

3 Experimental setup

In order to establish the test conditions in this research, firstly, the engine was started in gasoline mode at 1800 rpm engine speed (ES) and a CR of 10 to have it warmed up to a steady-state operating condition. The engine was then set to operate under full-load condition in gasoline mode (G100) at an ER of 0.9. Maintaining the operating conditions in terms of the ER (0.9), the SA was varied at a crack angle step of one or 2°CA, with 400 successive cycles recorded at each SA.

The raw recorded data was decomposed into successive cycles using a Fortran-coded program, so as to calculate the variations of $P - \theta$ (the in-cylinder pressure versus the crank angle) and *imep* for each cycle and evaluate average values over the cycles. Further measured were the inlet mixture temperature, ES, output torque, λ, and amounts of exhaust emissions (NO_x, HC, and CO) and temperature of the exhaust gases. Next, using the peak output torque and imepav obtained from the in-cylinder pressure, a free-knock optimum SA within the predefined non-knocking region was determined.

Continuing with the experiments, with the engine operating under full-load condition, three mass-based blends of the two fuels (G87.5, G75, and G62.5 containing gasoline at 87.5%, 75%, and 62.5%, respectively, with the remaining part being composed of NG) were separately applied to the engine. For each blend, different SAs were tested and the respective data was acquired. Similar to the case with pure gasoline as fuel, the cases with the blended fuel had their free-knock optimum SA determined based on the peak $imep_{av}$ and output torque in the non-knocking region.

A preliminary investigation of the results on this engine showed that, keeping constant the fuel injection period, a change in the SA would lead to only subtle changes in the recoded ER based on the analysis of the exhaust gases. Since the present work was aimed at investigating the efficiency of dual fuels at a constant ER of 0.9, at each SA, keeping the mass ratio of the pure fuels unchanged, the fuel injection periods were set to maintain the ER of the exhaust gases in the range of 0.9 ± 0.01.

In order to define the no-knocking region (i.e. the condition under which no sign of knocking was observed on the $P-\theta$ diagram), it was necessary to analyze and interpret the cycle knockings under various operating conditions. For this purpose, maximum amplitude of the pressure oscillations (MAPO) induced by the knocking was used as a measure of the knocking [?, ?]. In the relevant literature, the cycle for which the MAPO exceeds 1 bar is identified as susceptible to knocking, and should the percentage of the knocking cycles, KC, exceed 10% under a particular operating condition, the operating condition is recognized as knocking [?]. In the SI engines, in order to avoid such circumstances, the SA is retarded. We used the MAPO to define the non-knocking region in the present research, with the results described in the respective section. Once finished with data acquisition at a CR of 10, the engine was shut down and the CR was changed to 11 before repeating the mentioned procedure.

Two ideas can be followed to adjust the dual fuel supply: one is to find injection periods of the two fuels for achieving the given fractions and ER at an arbitrary SA, then preserving the injection periods for the other SAs. Second idea is to maintain the given fuel fractions and ER for each SA. The former was considered to collect data at CR of 10, in which the supplied fuel energies for all SAs can be identical; the later was followed to gather data at CR of 11, where ER of all SAs are the same.

4 Results and discussion

4.1 Diagnosis and definition of the non-knocking region

Based on the relevant studies in the literature, an operating condition is identified as knocking should the number of KC exceeds 10%. Accordingly, it can be implicitly inferred that a condition for which the number of the KC is zero defines a perfectly non-knocking condition. In this way, one could define a region between the knocking condition and the perfectly non- knocking condition, within which some 0-10% of the cycles render knocking. In the present work, this region is referred to as the transitional region or a borderline condition between the knocking and perfectly non- knocking conditions. Figure **??** demonstrates the variations of *imep* and the percentage of KC against the SA and the knocking, perfectly non-knocking, and transitional regions for G75 condition. In this study, in order to compare the engine performance at optimal SA for the respective fuel, tests were performed to keep the number of KC below 5%. Accordingly, for a given fuel composition and predefined operating conditions (CR, ES, and ER), the SA at which the $imep_{av}$ or the peak output torque was maximum was referred to as $non-adverseknockingoptimum$ SA (NAKOSA). Based on the studies performed in the present research, good agreements was observed between the variation trends of torque and $imep_{av}$ versus SA.

In order to clarify the adverse and non-adverse

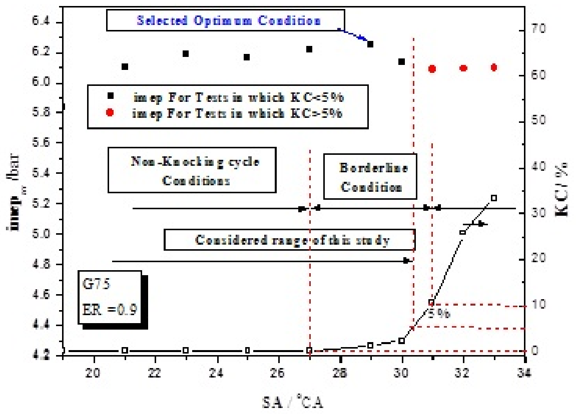

Figure 3: Variations of *imep* and percentage of KC against the SA and knocking, perfectly non-knocking and transitional regions for G75 condition.

knocking conditions based on the mentioned definition, among the pool of experiments performed with G75 as the fuel at a CR of 11, ES of 1800 rpm, and lean ER of 0.9, two experiments with knocking-cycle percentages of 10.5% and 2.25% relating to the SAs of 31 and 30°CA were selected. That is, only 1°CA of change in the SA has changed the condition from the transitional region to knocking region. Average value of the MAPO ($MAPO_{av}$) was calculated from the cycles recorded in each test followed by searching for the cycle with the closest MAPO value to the $MAPO_{av}$. Figure **??** shows the $P-\theta$ diagram of the representative cycles selected based on the $MAPO_{av}$ for the two tests with G75. On this figure, it is obvious that the difference in peak pressure between the two test was about 1.5 bar on as-recorded data (in presence of knocking). Sorting the data in the decreasing order of MAPO, the position of the two cycles was found to fall in the beginning of the second quarter of the total of 400 cycles. Knowing that the cycle representing the SA of 30°CA showed no obvious indication of knocking, it can be concluded that at least three-fourth of the respective cycles were free of significant knocking, which proves the normal combustion tendency of the respective test. However, symptoms of knocking were evident on the cycle representing the SA of 31A. Based on these reasons, it seems that the non-adverse knocking region assumed in this study (KC¡5%) or determining the optimal SA based on the peak *imep* was appropriate.

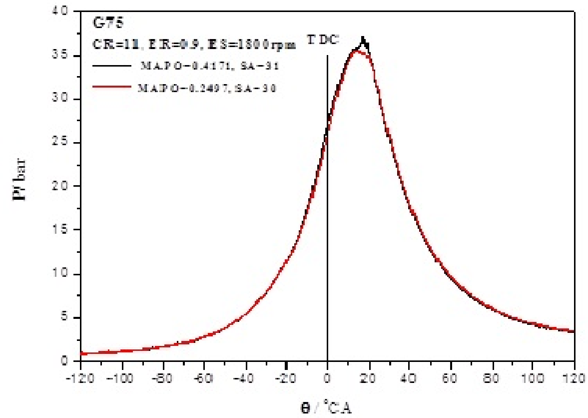

Figure 4: The $P-\theta$ diagrams of the cycles selected based on MAPOav for the two tests with G75

4.2 Discussion on the results

The experimental tests performed in the present work were performed using a single-cylinder research engine with four gasoline-NG dual fuels at two CRs of 10 and 11, an ES of 1800 rpm, and an ER of 0.9 under at least seven different SAs. For 400 successive cycles, variations of the in-cylinder pressure, output torque, exhaust emission fractions (HC, CO) were measured. Upon processing the $P-\theta$ data for each cycle, we could identify the knocking signals and smoothed in-cylinder pressure, MAPO, and nature of the knocking of each cycle, and then proceed calculate the percentage of KC and MAPOav for each test. Moreover, the P- data for the 400 successive cycles, the value of the ensemble average cycle (EAC) $P-\theta$ (averaging the in-cylinder pressure at different crank angles on the test cycles) was computed [?]. Figure ?? presents an example of the developed $P-\theta$ diagram for 400 successive cycles for the G75 fuel at a CR of 11 and SA of 30°CA along with the EAC value. Of the factors affecting the cyclic changes in the spark-ignition engines, one can refer to the cyclic variations in the turbulence rate of the cylinder chamber, air-to-fuel ratio, residual gas content, mixture heterogeneity within the chamber, especially in the vicinity of the ignition spark, and electrical discharge parameters of the spark plug [?]. Another important factor that may contribute to the present work is the non-uniformity of the distribution of gasoline and NG in the mixture within the cylinder. Therefore, although the preset operating conditions of the engine were kept unchanged, the synergetic effect of the mentioned factors made differences among the $P-\theta$ diagrams for the 400 successive cycles. These differences might impose changes into the cycle and IMEP. Considering the importance of the cyclic changes at lean ER, the cyclic variations of IMEP were evaluated at optimal spark advance at non-adverse knocking region for the respective cycles. Figure 6 reports the values of IMEP for each cycle against the cycle number for G100 and G75 fuels at the respective optimal spark advances and a compression ratio of 11. With the scales of the diagrams for the two fuels being identical, major differences in the cyclic variations are evident. The G75 showed significantly smaller divergence of the data points, as compared to G100. Accordingly, the maximum divergence from the average (absolute deviation from average) was 6.62% for G100 and about 4.87% for G75. Performing a statistical analysis on the data, it was found that the standard deviation (σ) of IMEP for the G100 and G75 fuel blends was 0.113 bar and 0.061 bar, respectively, reducing the COV from 1.84% to 0.98%. Since the aim of the present research was to evaluate and compare the efficiency of different fuel blends within the non-adverse knocking region, the safe optimal spark advance was obtained for different blends according to the explained procedure. In other words, for each fuel blend, using given values of the revolution speed, compression ratio, and ER, the experimental data was extracted at different spark advances and the value of $IMEP_{av}$ was used to find the optimal spark advance in the range of advances for which the percentage of knocking cycles was less than 5%. Figure ?? shows the procedure for selecting the

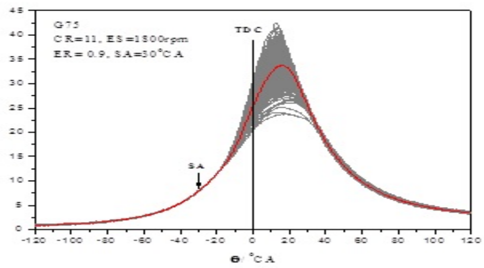

Figure 5: The $P-\theta$ diagram for 400 successive cycles along with a hypothetical equivalent cycles for the G75 fuel at a compression ratio of 11 and ER of 0.9.

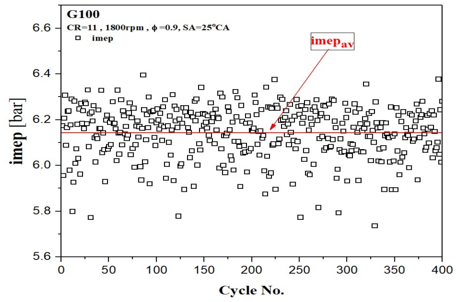

(a)

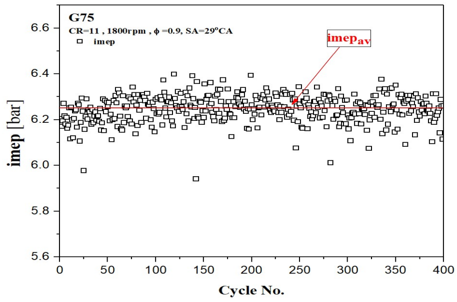

(b)

Figure 6: Variations of IMEP against the cycle number at optimal non-adverse knocking region for (a) G100 and (b) G75 fuel blends.

optimal type conditions in the non-knocking region.

Figure ?? shows the variations of the σ and COV of the IMEP for different fuel blends at the respective optimal spark advance. On this figure, it is evident that an increase in the fraction of the NG in the blend lowers the values of the and COV. Accordingly, at a compression ratio of 10, the percent decreases in the σ and COV with G62.5 rather than G100 were found to be about 37% and 36%, respectively. A major cause of such a significant decrease might be the gaseous nature of the NG, which facilitates its blending with other gases, including the air, contributing to the homogeneity of the NG distribution within the cylinder. The decreased difference in the cyclic variations with decreasing the gasoline fraction in the blend provided another proof for this fact. Figure ?? shows the

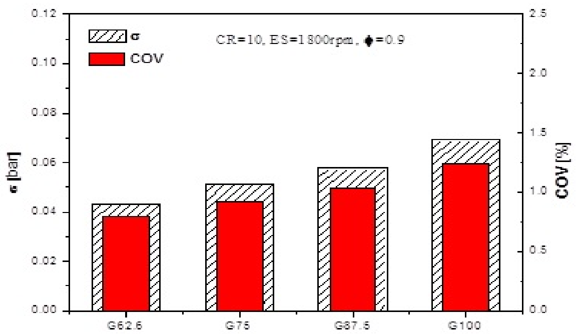

Figure 7: Variations of the σ and COV for G100, G87.5, G75, and G62.5 at respective optimal spark advances for compression ratios of 10

variations of IMEPav as a function of the percentage of gasoline in the blended fuel at the respective optimal spark advance at the two compression ratios at identical revolution speed and ER. Since the values over 400 successive cycles were used to evaluate the IMEPav, the results were of good accuracy. The results show that, at CR=10, with decreasing the fraction of gasoline down to G75, the IMEPav showed no significant change. However, upon further decreasing the share of gasoline to G62.5, the value of $IMEP_{av}$ decreased slightly due to the adverse effects of the gas on the volumetric efficiency and the available energy through the cycle. At CR = 11, for G = 100, due to the possible heterogeneity of the gasoline content of the blend (as mentioned above), some reduction in the respective $IMEP_{av}$ was observed. The trend of results for G62.5 was similar to that at CR = 10. At the studied ER, the G75 and G87.5 exhibited desirable values of $IMEP_{av}$. Figure ?? shows the variations in the

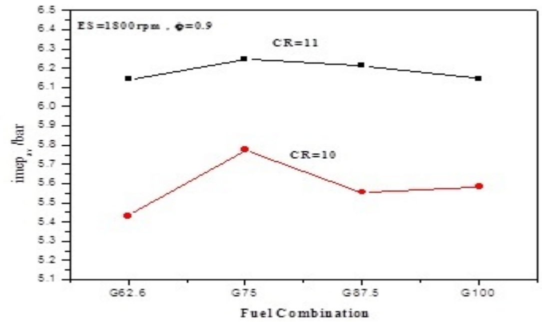

Figure 8: The values of $IMEP_{av}$ for G100, G87.5, G75, and G62.5 at respective optimal spark advances for compression ratios of 10 and 11

fractions of HC and CO in the exhaust gas for different percent shares of gasoline in the studied blended fuels under safe optimal spark advance condition at two compression ratios. It is herein observed that, under the optimal condition, both the HC and CO fractions decrease with increasing the compression ratio from 10 to 11. The reason behind this trend can be the high temperature and pressure and hence lowered fraction of residual gas thanks to the increased compression at combustion, which is known to contribute to higher burning rate and the chances of complete combustion of contents of the cylinder. Moreover, it was observed that nearly the same amounts of HC and CO were found in the exhaust gas produced by both G87.5 and G75 regardless of the

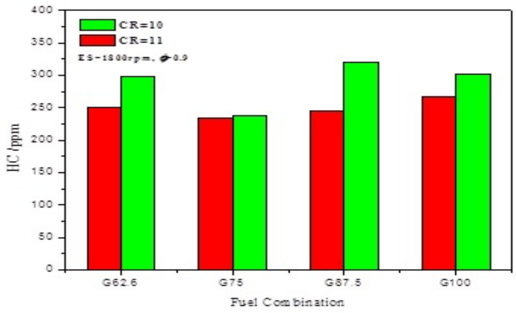

(a)

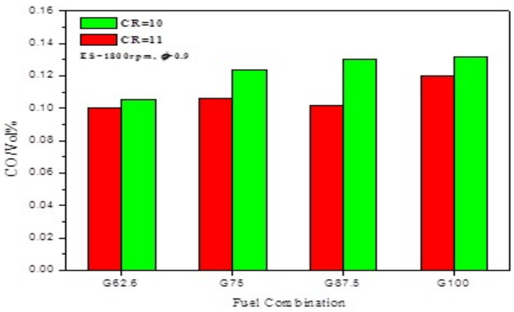

(b)

Figure 9: Variations of the percent fractions of (A) HC and (B) CO in the exhaust gas for different percent shares of gasoline in the studied blended fuels under safe optimal condition at two compression ratios.

compression ratio, with the amounts decreased by about 27% and 19% with increasing the compression ratio, respectively. The emission reduction was minimal (10%) for HC with G100 as fuel. With G62.5 as the fuel, the fraction of CO was minimal at both compression ratios, with the respective reduction of 7%.

5 Conclusion

In the present work, four different blends (G100, G87.5, G75, and G62.5) of gasoline and natural gas were experimentally investigated in a single-cylinder spark-ignition engine at CRs of 10 and 11, an ER of 0.9, and a revolution speed of 1800 rpm. Upon analyzing the data from 400 successive cycles for each test, the following remarks and conclusions were drawn:

In this study, the entire spectrum of feasible spark advances was divided into three sub regions, namely knocking region (%KC > 10), transitional or marginal region (0 < %KC<10), and perfectly non-knocking region (% KC = 0). The safe non-adverse knocking condition was defined as %KC < 5, and the knocking-safe optimal spark advance was considered to achieve maximal IMEP or output torque.

Investigating the variations of the and COV of the IMEP for different fuel blends, it was observed that, with increasing the percent fraction of NG in the fuel blend, both the and COV decreased. Accordingly, at CR = 10, the mentioned parameters for G62.5 were some 36 It was implicitly observed that, for blended fuels, non-uniform distribution of each fuel within the cylinder can serve as a new source for cyclic variations.

Under the considered lean burning condition at optimal safe spark advance, the IMEP and output torque for the gas-contained fuel blends were comparable to those obtained by the pure gasoline.

Investigating the exhaust gases, including HC, CO, at both compression ratios (CR = 10, 11), it was observed that an increase in the compression ratio reduced the emitted amounts of all two pollutants. The percent fractions of HC and CO for the G87.5 and G75 fuel blends were almost equal to one another at either of the studied compression ratios, with their values decreased by about 27% and 19%, respectively, with increasing the compression ratio. The reduction in HC with increasing the compression ratio was minimal for G100 (10%) With G62.5 as the fuel, the fraction of CO was minimal at both compression ratios, with the respective reduction of 7% With G62.5 as the fuel, the fraction of CO was minimal at both compression ratios, with the respective reduction of 7%.

Investigating the engine performance and emission characteristics, the G75 was found to be the optimal blended fuel at a compression ratio of 11, as compared to the other blends considered in this work.

References

[1] A. H. Kakaee, A. Paykani, Research and development of natural-gas fueled engines in Iran, *Renewable and Sustainable Energy Reviews* 26 (2013) 805-821.

[2] B. Petroleom, BP Statistical Review of World Energy, bp.com/statisticalreview (2015).

[3] H. M. Cho, H. Bang-Quan, Spark ignition natural gas engines a review, *Energy Convers Manage* 48 (2007) 608-618.

[4] M. I. Jahirul, H. H. Masjuki, R. Saidur, M. A. Kalam, M. H. Jayed, M. A. Wazed, Comparative engine performance and emission analysis of CNG and gasoline in a retrofitted car engine, *Appl Therm Eng.* 30 (2010) 2219-2226.

[5] M. A. Kalam, H. H. Masjuki, An experimental investigation of high performance natural gas engine with direct injection, *Energy* 36 (2011) 3563-3571.

[6] M. Sarabi, E. Abdi Aghdam, Experimental analysis of in-cylinder combustion characteristics and exhaust gas emissions of gasolinenatural gas dual-fuel combinations in a SI engine, *Journal of Thermal Analysis and Calorimetry*. http://dx.doi.org/10.1007/s10973-019-08727-2/

[7] R. Behrad, E. Abdi Aghdam, Experimental study of knocking phenomenon in different gasoline-natural gas combinations with gasoline as the predominant fuel in a SI engine, *Journal of thermal analysis and calorimetry*. http://dx.doi.org/10.1007/s10973-019-08579-w/.

[8] Z. Ran, D. Hariharan, B. Lawler, S. Mamalis, Experimental study of lean spark ignition combustion using gasoline, Ethanol, Natural gas, syngas, *Fuel* 235 (2019) 530-537.

[9] Asiah Ab. Rahim, N. Rosli Abdullah, Effect of alcohol-gasoline blends (ethanol) on performance and emission of si engine, *ARPN Journal of Engineering and Applied Sciences* 11 (2016) 416-429.

[10] A. Piknas, P. Saugirdas, G. Juozas Grabys, Influence of composition of gasoline ethanol blends on parameters of internal combustion engines, *Journal of KONES Internal Combustion Engines* 10 (2003) 3-4 .

[11] [11] Y. Xiumin, G. Zezhou, H. Ling, D. Wei, S. Ping, SH. Weibo, D. Yaodong, H. Fengshuo, Effect of gasoline/n-butanol blends on gaseous and particle emissions from an SI direct injection engine, *Fuel* 229 (2018) 110.

[12] E. Pipitone, S. Beccari, Performances and emissions improvement of an SI engine fuelled by LPG/gasoline mixtures (No. 2010-01-0615), *SAE Technical Paper*.

[13] E. Pipitone, S. Beccari, Performances improvement of a S. I. CNG bi-fuel engine by means of double-fuel injection, *SAE Technical Paper* 24 (2009) 24-58.

[14] MM. Movahed, HB. Tabrizi, M. Mirsalim, Experimental investigation of the concomitant injection ofgasoline and CNG in a turbocharged spark ignition engine, *Energy conversion and management* http://dx.doi.org/10.1016/j.enconman.2014.01.017/

[15] D. Ramasamy, C. Y. Goh, K. B. Kadirgama, F. Benedict, M. M. Noor, G. Najafi, A. P. Carlucci, Engine performance, exhaust emission and combustion analysis of a 4-stroke spark ignited engine using dual fuel injection, *Fuel* 207 (2017) 719-728.

[16] S. Di lorio, P. Sementa, B. M. Vaglieco, F. Catapano, An experimental investigation on combustion and engine performance and emissions of a methane-gasoline dual-fuel optical engine (No. 2014-01-1329). *SAE Technical Paper*.

[17] CH. Gong, L. Zhaohui, CH. Yulin, L. Jiajun, L. Fenghua, H. Yongqiang, Influence

of ignition timing on combustion and emissions of a spark-ignition methanol engine with added hydrogen under lean-burn conditions, *Fuel* http://dx.doi.org/10.1016/j.fuel.2018.07.097/

[18] S. Di lorio, P. Sementa, B. M. Vaglieco, F. Catapano, An experimental investigation on combustion and engine performance and emissions of a methane-gasoline dual-fuel optical engine (No. 2014-01-1329), *SAE Technical Paper.*

[19] E. Abdi Aghdam, M. Bashi, Effectiveness of performance characters of a SI engine by varying injection start position of gasoline and natural gas fuels, *Modares Mechanical Engineering* 15 (2015) 134-142.

[20] M. Ghorbanzadeh, The effect of different fuels (gasoline natural gas) on cyclic variations of a spark ignition engine running on lean mixture, *Modares Mechanical Engineering* 13 (2013) 101-108.

[21] M. Sarabi, E. Abdi-Aghdam, S. K. Yekani, The Effect Of Burned Residual Gases On Gasoline-NG Dual-Fuel Engine Combustion Performance With Skip-Fire Technique, *The Journal of Engine Research* 23 (2021) 3-11.

[22] E. Abdi Aghdam, M. Sarabi, M. Khomeyrani, Experimental study of laminar burning velocity for dual fuel (Gasoline-NG)-Air mixture using pressure record in a spherical combustion bomb at higher primary pressure, *Fuel and Combustion* 11 (2018) 121-134.

[23] F. FAmrouche, P. Erickson, S. Varnhagen, J. W. Park, An experimental analysis of hydrogen enrichment on combustion characteristics of a gasoline Wankel engine at full load and lean burn regime, *International Journal of Hydrogen Energy.* http://dx.doi.org/10.1016/j.ijhydene.2018.08.110/

[24] X. Duan, L. Yangyang, L. Jingping, G. Genmiao, F. Jianqin, Experimental study the effects of various compression ratios and spark timing on performance and emission of a lean-burn heavy-duty spark ignition engine fueled with methane gas and hydrogen blends, *Energy.* http://dx.doi.org/10.1016/j.energy.2018.12.029/

[25] E. Abdi Aghdam, M. Ataee Tarzanagh, The Effect of Burned Residual Gases on Optimum Ignition Timing using Skip Fire Technique, *JER.* 50 (2018) 67-75

[26] MA. Ceviz, AK. Sen, AK. Kuleri, Engine performance, exhaust emissions, and cyclic variations in a lean-burn SI engine fueled by gasolinehydrogen blends, *Appl. Therm. Eng.* http://dx.doi.org/10.1016/j.applthermaleng.2011.10.039/

Seyyd Kazem Yekani is a PhD in Department of Mechanical Engineering, Faculty of Engineering, University of Mohaghegh,Ardabili, Ardabil, Iran. His research interests spark ignition enginein lean-burn condition.

Ebrahim Aabdi Aghdam is Professor of mechanical engineering in Department of Mechanical Engineering, Faculty of Engineering, University of Mohaghegh Ardabili, Ardabil, Iran. His research interests include numerical and experimental investigation of the performance response of a spark ignition engine. He received his Ph.D. from University of Leeds, UK in 2001.

Mehrdad Sarabi is a PhD in Department of Mechanical Engineering, Faculty of Engineering, University of Mohaghegh Ardabili, Ardabil, Iran. His research interests spark ignition engine in dual-fuel condition.